Electronic Supplementary Information (ESI)

Core-shell metal-macrocycle framework (MMF): spatially selective dye inclusion through core-to-shell anisotropic transport along crystalline 1D-channels connected by epitaxial growth

Shohei Tashiro,*[a] Shinya Mitsui,[a] David W. Burke,[a] Ryou Kubota,[a] Nobuyuki Matsushita[b] and Mitsuhiko Shionoya*[a]

[a]*Department of Chemistry, Graduate School of Science, The University of Tokyo, 7-3-1 Hongo, Bunkyo-ku, Tokyo 113-0033, Japan*

[b]*Department of Chemistry, College of Science and Research Center for Smart Molecules, Rikkyo University, Nishi-ikebukuro, Toshima-ku, Tokyo 171-8501, Japan*

Materials and methods

Macrocyclic ligand **L** was synthesised according to our previous procedure.[1] The preparation and the crystal structure of MMF-Cl were previously developed by us.[1] Other reagents including solvents, organic and inorganic compounds are commercially available, and were used without further purification.

Single-crystal X-ray crystallographic analyses were carried out using a Rigaku XtaLAB P200 diffractometer with CuKα or MoKα radiation, and the obtained data were analysed using a CrystalStructure crystallographic software package or Olex-2 crystallographic software package except for refinement, which was performed using SHELXL version 2018/3.[2] X-ray structures were displayed using a Mercury program. Powder X-ray diffraction measurement was conducted using a Rigaku SmartLab diffractometer with CuKα radiation. ^{1}H NMR spectra were recorded on a Bruker AVANCE 500 spectrometer (500 MHz) and calibrated with the signal of $(CD_2H)CD_3SO$ at 2.50 ppm. Single-crystal absorption spectra were collected using a microspectrophotometer consisting of a fiber-optic spectrometer (Ocean Optics Inc., USB 2000) and a microscope (Olympus, BX51) equipped with a tungsten lamp for transmission illumination. Raman spectroscopy was performed using a JASCO NRS-5100 micro-Raman spectrometer with an optical density filter (O.D. = 2). A 532 nm laser was used for Raman spectroscopic measurements. XPS measurements were carried out using PHI5000 VersaProbe (ULVAC-PHI) with AlKα radiation. The hemispherical electron energy analyser was operated at a pass energy of 23.5 eV, and all measurements were conducted using a neutraliser. Elemental analysis was carried out using an Elementar Vario Micro cube. The plot profile of luminance (gray value) was generated using an ImageJ program.

Preparation of MMF-Cl and MMF-Br

• *MMF-Cl*[1]

Acetonitrile solutions of macrocyclic ligand **L** and $PdCl_2(CH_3CN)_2$ were mixed at 80 °C so that the concentration of the mixture was adjusted to [**L**] = 0.28 mM and $[PdCl_2(CH_3CN)_2]$ = 0.91 mM. Yellow platelet MMF-Cl crystals were obtained after leaving this mixture to stand at room temperature for several days. The crystal data obtained by single crystal X-ray diffraction measurements was well consistent with the previous data.[1]

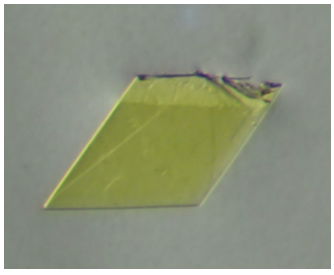

Figure S1. Picture of an MMF-Cl crystal.

• *MMF-Br*

Acetonitrile solutions of macrocyclic ligand **L** and $PdBr_2(CH_3CN)_2$ were mixed at 80 °C so that the concentration of the mixture was adjusted to [**L**] = 0.29 mM and [$PdBr_2(CH_3CN)_2$] = 1.3 mM. Orange platelet MMF-Br crystals were obtained after leaving this mixture to stand at room temperature. After 2 weeks, the resulting orange crystals were collected, washed with CH_3CN and air-dried for several hours to isolate MMF-Br, $(Pd_3\mathbf{L}Br_6)\cdot(CH_3CN)_{0.14}\cdot(H_2O)_9$, in 59% yield. The chemical composition of the resulting crystals was determined by ^1H NMR measurement of the crystals dissolved in DMSO-d_6/DCl-D_2O and elemental analysis. The phase purity of MMF-Br dispersed in CH_3CN was confirmed by powder X-ray diffraction using a glass capillary. For single-crystal X-ray diffraction measurement, MMF-Br crystals similarly prepared were peeled off from the glass vial by replacing the solution with acetone, and then one of the crystals was analysed.

Elemental analysis: calcd for $C_{42}H_{42}N_6Br_6Pd_3\cdot(H_2O)_9\cdot(CH_3CN)_{0.14}$: C 31.79, H 3.81, N 5.38; found: C 31.87, H 3.67, N 5.20.

Crystal data for $(Pd_3\mathbf{L}Br_6)_2\cdot(CH_3CN)_{1.5}\cdot(CH_3COCH_3)_{1.71}\cdot(H_2O)_{1.75}$: $C_{92.11}H_{98.73}Br_{12}N_{13.5}O_{3.46}Pd_6$, F_w = 3047.55, crystal dimensions 0.150 × 0.090 × 0.070 mm^3, monoclinic, space group $P2_1/c$, a = 20.00896(19), b = 53.1688(5), c = 14.50409(14) Å, β = 88.4818(8)°, V = 15424.8(3) Å^3, Z = 4, ρ_{calcd} = 1.312 g cm^{-3}, μ = 94.53 cm^{-1}, T = 93 K, λ(CuKα) = 1.54184 Å, $2\theta_{max}$ = 147.178°, 100397/30274 reflections collected/unique (R_{int} = 0.0572), R_1 = 0.0834 ($I > 2\sigma(I)$), wR_2 = 0.2582 (for all data), GOF = 1.051, largest diff. peak and hole 2.198/–1.619 eÅ^{-3}. CCDC deposit number 1912584.

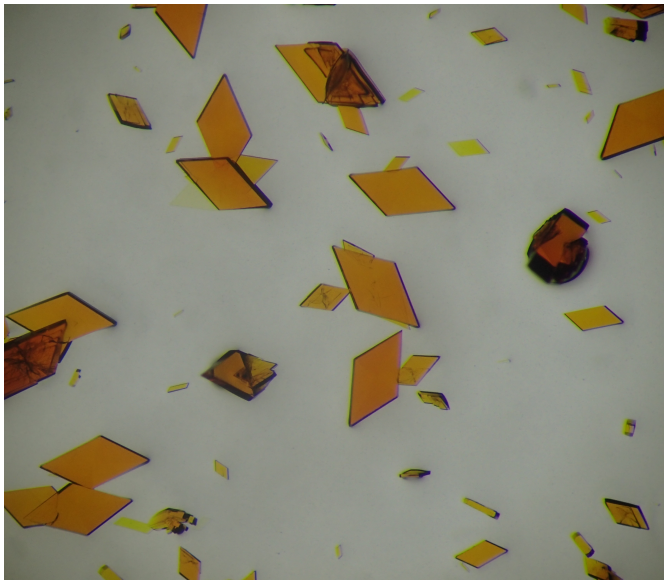

Figure S2. Picture of MMF-Br crystals.

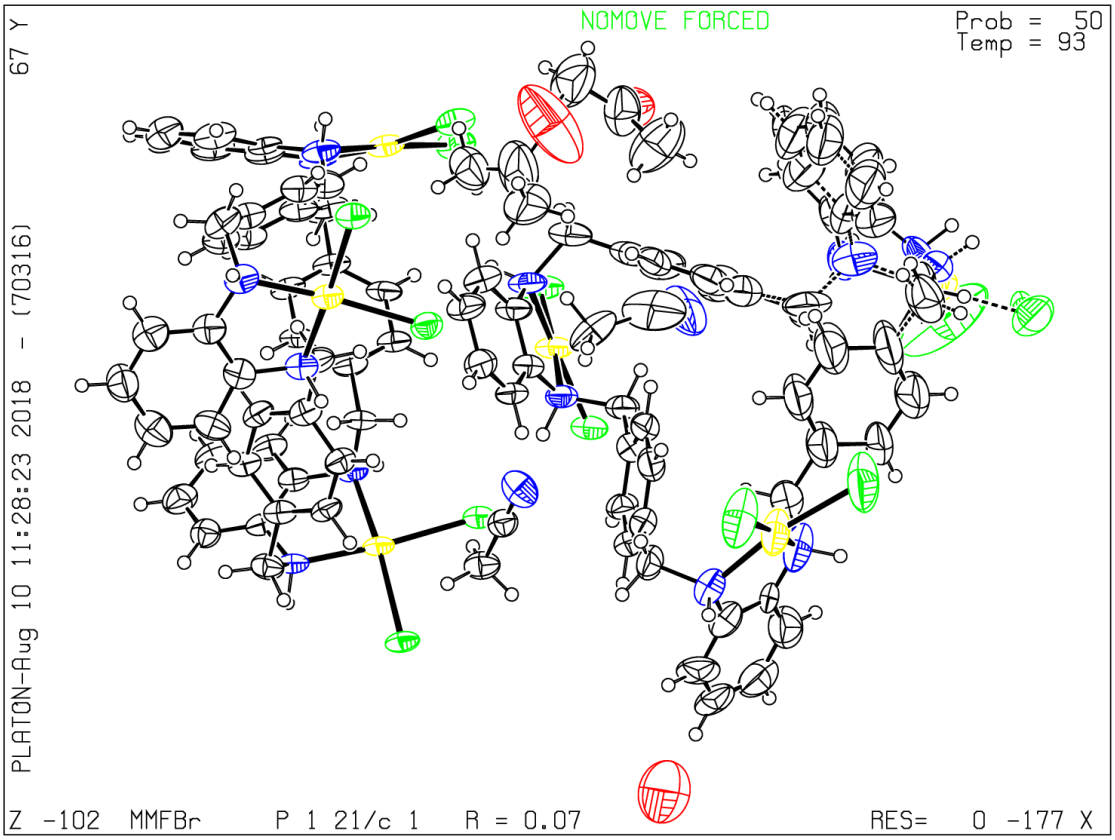

Figure S3. ORTEP drawing of MMF-Br at the 50% probability level. Color: C black, N blue, O red, Br green and Pd yellow.

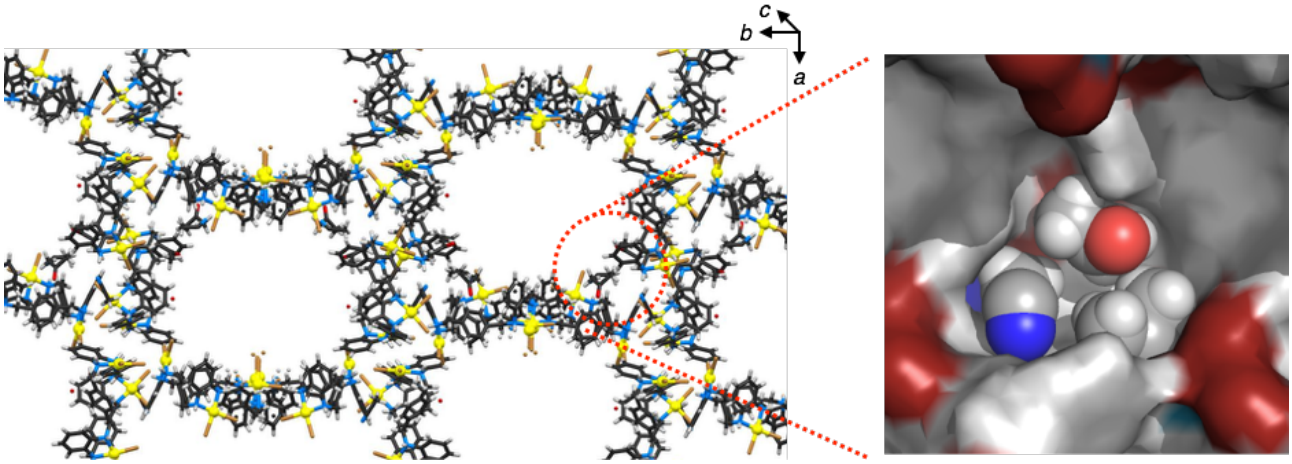

Figure S4. Crystal packing structure of MMF-Br (left) and the binding structures of solvents (acetonitrile and acetone molecules) at the bottom corner pocket (right).

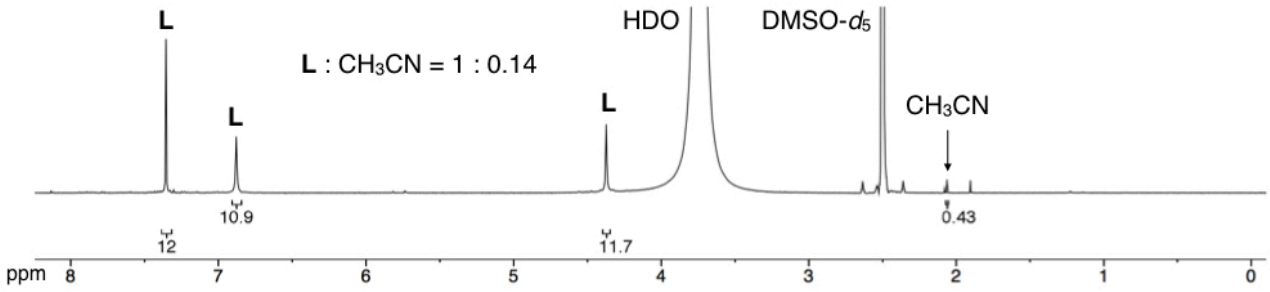

Figure S5. ^{1}H NMR spectra (500 MHz, DMSO-d_6, 300 K) after dissolving MMF-Br crystals in DMSO-d_6/DCl-D_2O.

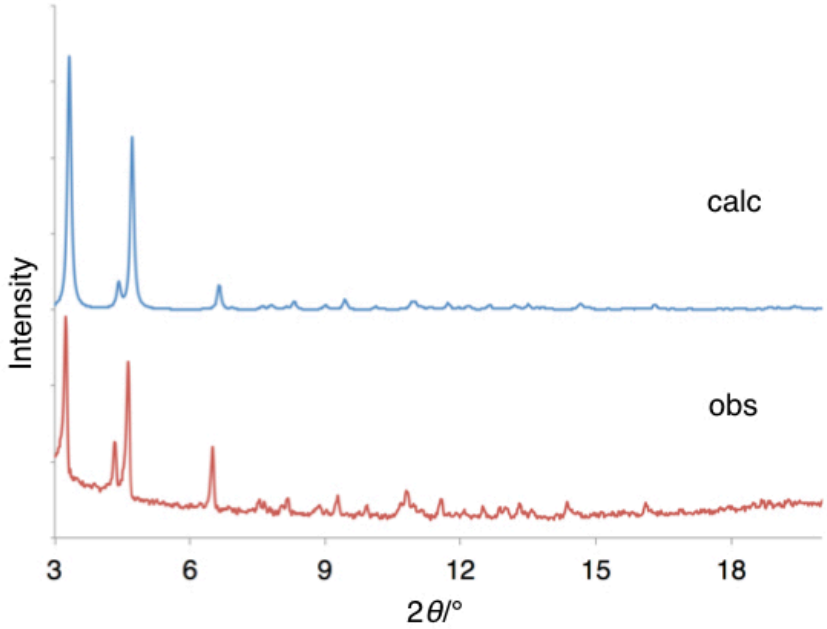

Figure S6. Powder X-ray diffraction patterns (CuKα, rt) of MMF-Br dispersed in CH_3CN (obs) and simulated from the crystal structure (calc).

Preparation of core-shell MMF-Cl@MMF-Br crystals

Acetonitrile solutions of macrocyclic ligand **L** and $PdCl_2(CH_3CN)_2$ were mixed at 80 °C so that the concentration of the mixture was adjusted to [**L**] = 0.28 mM and [$PdCl_2(CH_3CN)_2$] = 0.91 mM. Yellow platelet MMF-Cl crystals were obtained after leaving this mixture to stand at room temperature for one day. The resulting crystals were washed with acetonitrile by decantation and then mixed with an acetonitrile solution of macrocyclic ligand **L** and $PdBr_2(CH_3CN)_2$ ([**L**] = 0.28 mM, [$PdBr_2(CH_3CN)_2$] = 1.20 mM) prepared at 80 °C. Core-shell MMF-Cl@MMF-Br crystals were obtained after leaving this mixture to stand at room temperature for several days.

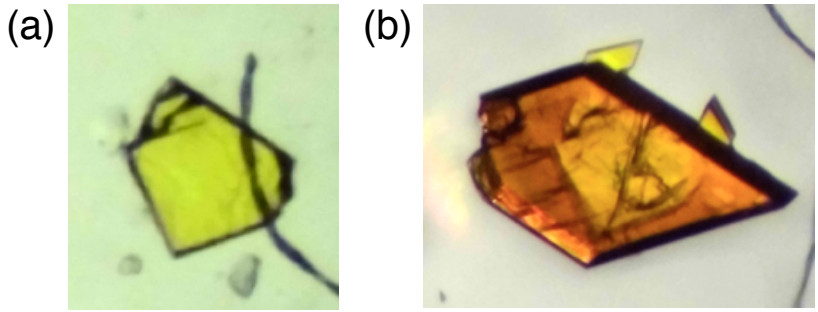

Figure S7. Pictures of (a) a seed MMF-Cl crystal and (b) an MMF-Cl@MMF-Br crystal.

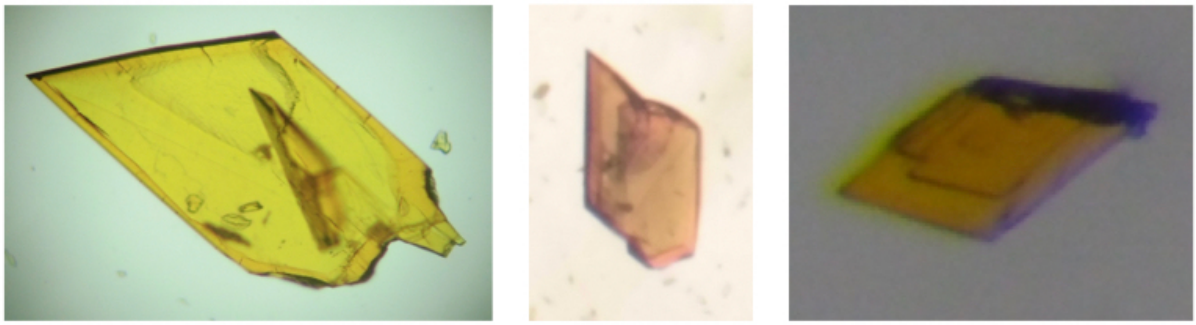

Figure S8. Pictures of MMF-Cl@MMF-Br crystals separately prepared by similar procedures.

Alternatively, an acetonitrile/methanol mixed solution was used for the crystallisation of seed MMF-Cl crystals to prepare thicker core-shell MMF-Cl@MMF-Br as described below. Acetonitrile/methanol (8:2) mixed solutions of macrocyclic ligand **L** and $PdCl_2(CH_3CN)_2$ were mixed at 80 °C so that the concentration of the mixture was adjusted to [**L**] = 0.28 mM and [$PdCl_2(CH_3CN)_2$] = 0.91 mM. Yellow block MMF-Cl crystals were obtained after leaving this mixture to stand at room temperature for one day. The resulting crystals were washed with acetonitrile by decantation, and then a mixed acetonitrile solution of macrocyclic ligand **L** and $PdBr_2(CH_3CN)_2$ ([**L**] = 0.28 mM, [$PdBr_2(CH_3CN)_2$] = 1.20 mM) was added to the on-growing MMF-Cl crystals. Core-shell MMF-Cl@MMF-Br crystals were obtained after leaving this mixture to stand at room temperature for several days.

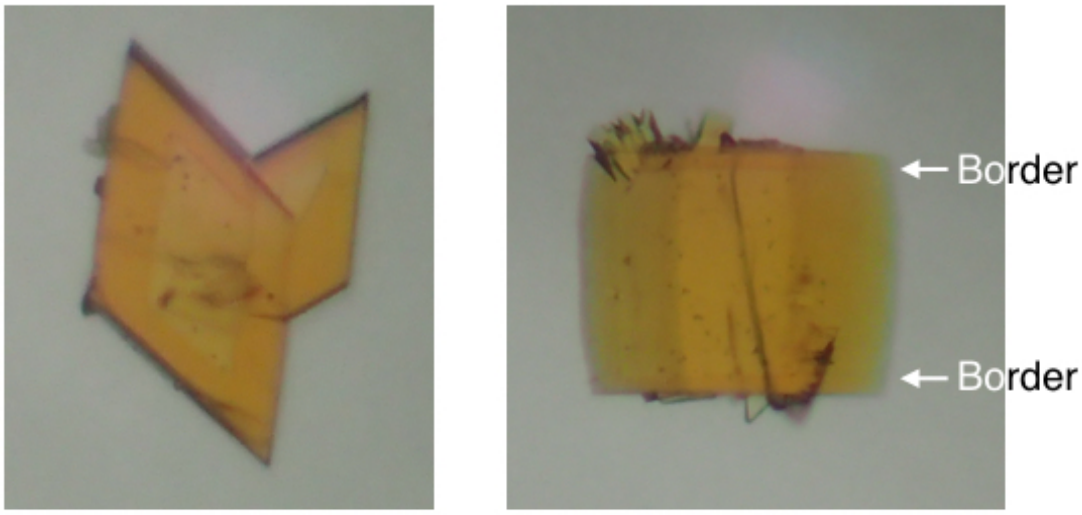

Figure S9. Pictures of thicker core-shell MMF-Cl@MMF-Br crystals from the top (left) and the side (right).

Attempts to prepare reverse core-shell MMF-Br@MMF-Cl crystals

Acetonitrile solutions of macrocyclic ligand **L** and $PdBr_2(CH_3CN)_2$ were mixed at 80 °C so that the concentration of the mixture was adjusted to [**L**] = 0.28 mM and [$PdBr_2(CH_3CN)_2$] = 1.20 mM. Orange platelet MMF-Br crystals were obtained after leaving this mixture at room temperature for one day. The resulting crystals were washed with acetonitrile by decantation, and then a mixed acetonitrile solution of macrocyclic ligand **L** and $PdCl_2(CH_3CN)_2$ ([**L**] = 0.28 mM, [$PdCl_2(CH_3CN)_2$] = 0.91 mM) was added to the growing MMF-Br crystals. In most cases, no core-shell crystals were obtained, though the formation of the target core-shell structure was observed only once, suggesting that this is not the best procedure for preparing the reverse core-shell structures reproducibly.

Characterisation of core-shell MMF-Cl@MMF-Br

• *Single-crystal absorption spectra*

Crystals in water were placed on the stage of an optical microscope. Transmission absorption measurements were performed on a crystal at room temperature.

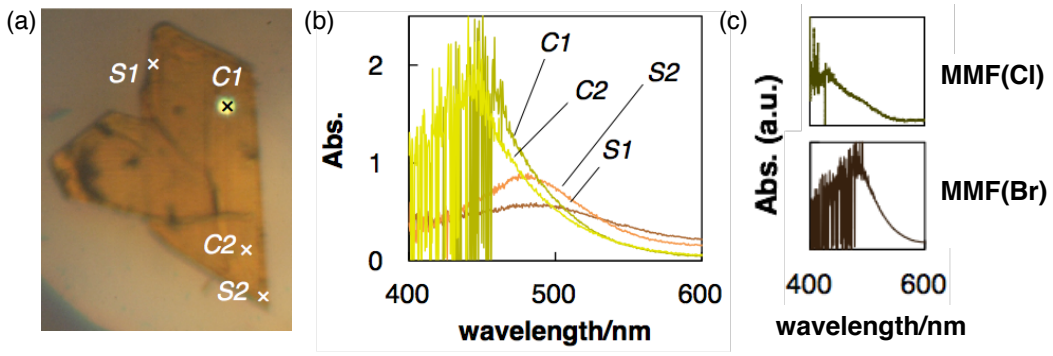

Figure S10. (a) A picture of a core-shell MMF-Cl@MMF-Br crystal with markers indicating the analysed positions on the crystal (*S1*, *S2*: shell, *C1*, *C2*: core). (b) Transmission absorption spectra of each indicated location on the core-shell crystal. (c) Transmission absorption spectra of MMF-Cl or MMF-Br crystals. Note that in our microspectroscopic system, the intensity of near-UV light shorter than 450 nm is very weak. In the case of absorbance more than 1.5, the signal of the light transmitted through the crystals is comparable with noise in this wavelength region. Therefore, the spectra of *C1* and *C2* are very noisy at wavelengths shorter than 450 nm.

• *Raman spectra*

Crystals were placed on the stage of an optical microscope installed in the spectrometer. Microscopic Raman measurements were performed on a crystal at room temperature.

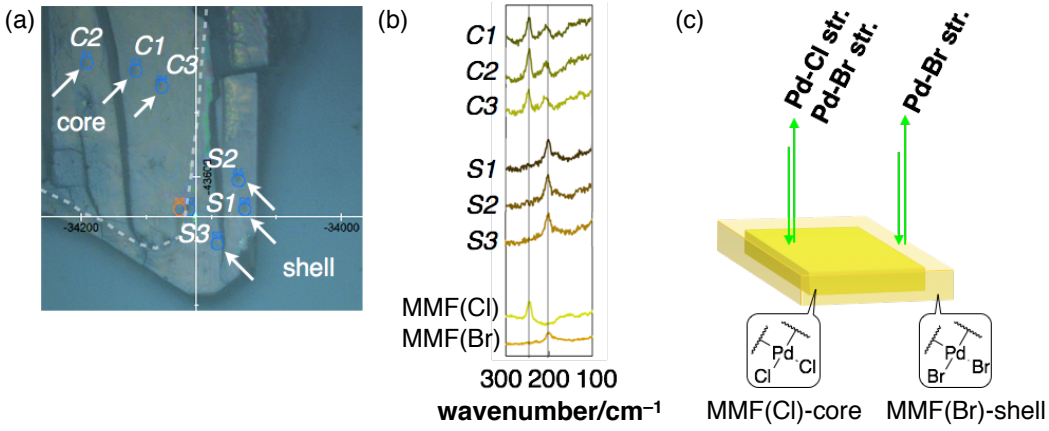

Figure S11. (a) A picture of a core-shell MMF-Cl@MMF-Br crystal with markers showing analysed places (*S1–S3*: shell, *C1–C3*: core). (b) Magnified Raman spectra of the core part and the shell part, MMF-Cl and MMF-Br, respectively. (c) Schematic diagram of the resulting core-shell crystal, in which the core is fully wrapped with the shell crystal, proven by Raman spectroscopy.

• *XPS*

Core-shell MMF-Cl@MMF-Br crystals were mounted on carbon tape attached to a sample holder and dried in vacuo for 2 h. Before measurements, the crystal surface was cleaned by Ar ion sputtering, and then scanning X-ray imaging was conducted to obtain an image of the crystal. The core and shell parts were analysed with a narrow X-ray beam with a diameter of 18 μm (Figure S12). The crystal was then further sputtered about fifty times, and each part was analysed again; however, the result was similar to Figure S12.

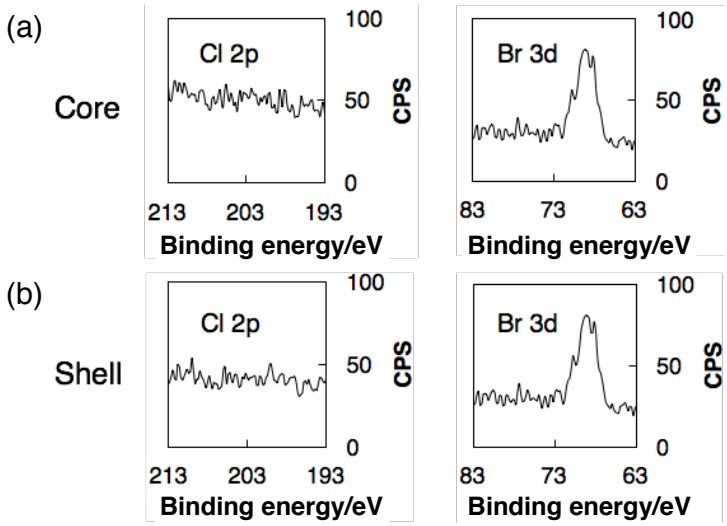

Figure S12. Magnified XPS spectra (Cl 2p and Br 3d components) of the surfaces of (a) core and (b) shell parts.

• *Single-crystal XRD analyses of each domain*

A core-shell crystal, MMF-Cl@MMF-Br, was immersed in glycerol to prevent drying and then cleaved with a micro-knife. The cut shell crystal was picked up for single-crystal XRD measurements. Next the remaining core-shell crystal was further cleaved to cut out a core piece, which was next picked up to measure single-crystal XRD. Although the quality of the crystal data was moderate due to the small size and cracking of the crystals obtained by this method, we were able to determine the structures based on the clear diffraction images. The lattice parameters of each domain were also determined based on the diffraction patterns. Notably, the lattice parameters of the core MMF-Cl crystal (a = 20.2300(9), b = 53.5168(16), c = 14.3304(3) Å) were significantly larger than those of pristine MMF-Cl (a = 19.5910(8), b = 51.730(3), c = 14.2715(10) Å), and were almost comparable to those of the MMF-Br shell crystal (a = 20.0078(3), b = 53.0768(9), c = 14.55750(18) Å). This lattice expansion of the MMF-Cl core crystal suggests that either the core structure is strained by the shell crystal with larger lattices, or the Cl^- ligands of the core are partially replaced with Br^- ligands.

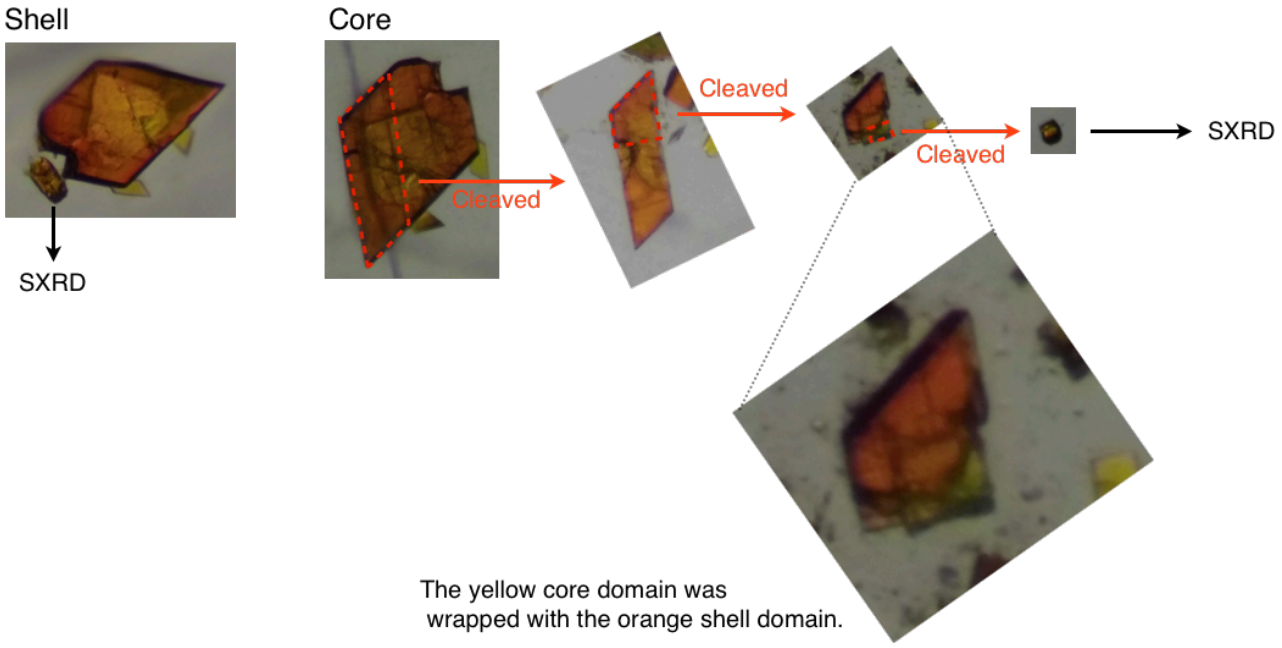

Figure S13. Schematic representation of the cleavage of a core-shell crystal (SXRD = single-crystal X-ray diffraction).

Crystal data of the shell (MMF-Br)

Crystal data for $(Pd_3LBr_6)\cdot(Pd_3LBr_{4.87}Cl_{1.13})\cdot(CH_3CN)_3\cdot(H_2O)$: $C_{90}H_{93}Br_{10.86}Cl_{1.14}N_{15}OPd_6$, F_w = 2947.42, crystal dimensions 0.147 × 0.085 × 0.071 mm^3, monoclinic, space group $P2_1/c$, a = 20.0078(3), b = 53.0768(9), c = 14.55750(18) Å, β = 91.3840(10)°, V = 15454.8(4) Å^3, Z = 4, ρ_{calcd} = 1.267 g cm^{-3}, μ = 3.545 mm^{-1}, T = 93 K, λ(MoKα) = 0.71073 Å , $2\theta_{max}$ = 55.0°, 124177/34507 reflections collected/unique (R_{int} = 0.0493), R_1 = 0.1090 ($I > 2\sigma(I)$), wR_2 = 0.3017 (for all data), GOF = 1.102, largest diff. peak and hole 4.143/–4.342 eÅ^{-3}. CCDC deposit number 1912586.

Note that, since the reflection intensities of the higher angle region were weak, the benzene rings of the *anti*-isomer were treated as rigid groups and restraints for thermal parameters such as SIMU and DELU were applied to the *anti*-isomer to avoid the collapse of the structure during refinement. To discuss the degree of halogen exchange on each Pd ion, some halogen atoms were analysed as disordered structures of Cl and Br. In contrast, six halogen atoms on the *syn*-isomer and two halogen atoms on the *anti*-isomer were analysed as Br atoms, because FVAR parameter optimization during refinement did not suggest any disorder models of Br and Cl. Hydrogen atoms of water molecules could not be located in the difference electron density maps.

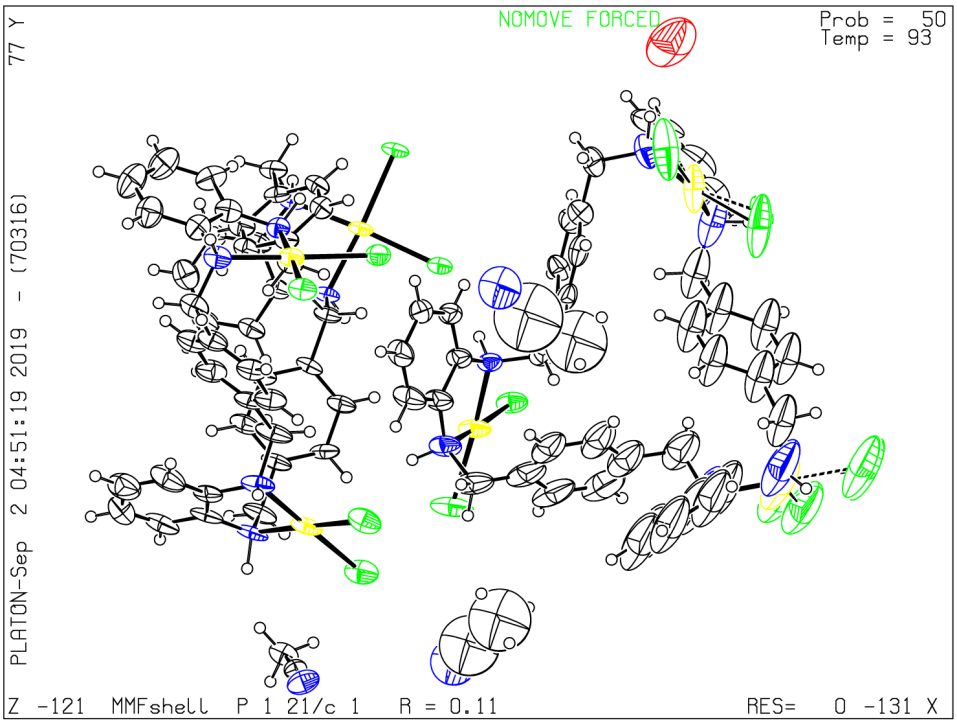

Figure S14. ORTEP drawings of the shell (MMF-Br) (50% probability level). Color: C black, N blue, O red, Br/Cl green and Pd yellow.

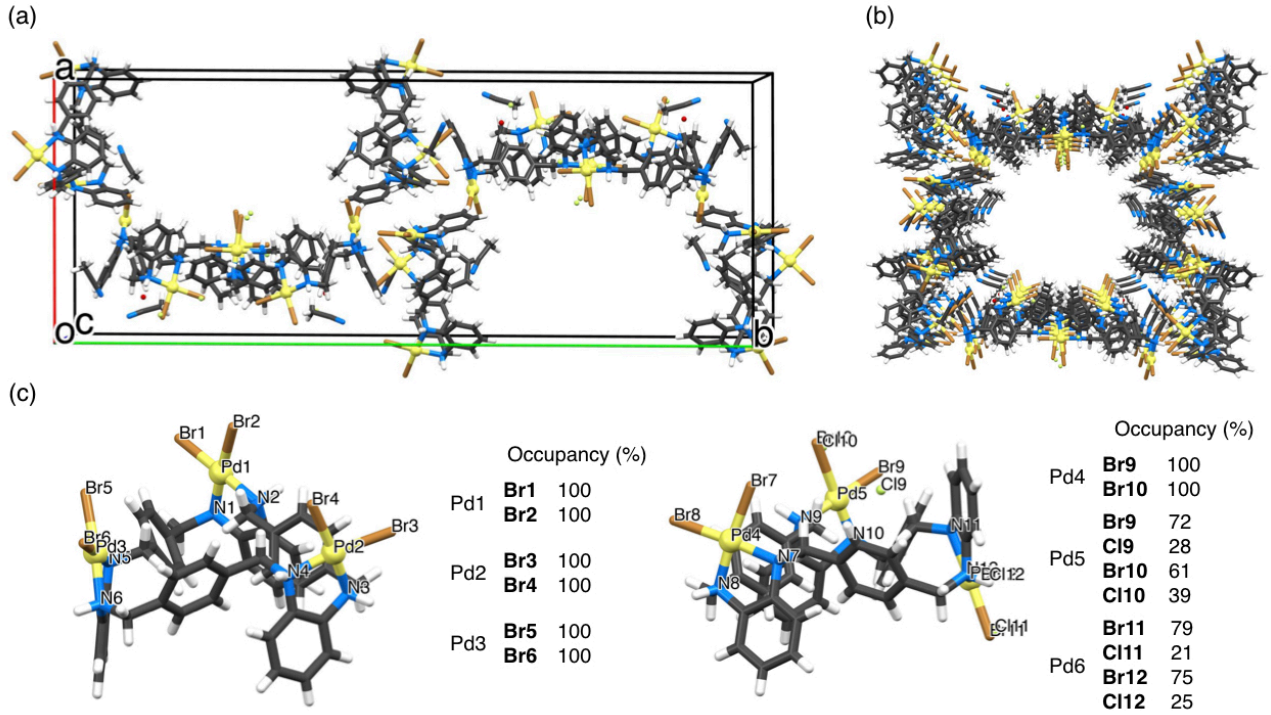

Figure S15. (a) Unit cell and (b) nano-channel structures of the shell (MMF-Br). (c) The *syn*- and *anti*-isomers and occupancy of halogen atoms on each Pd atom. Color: H white, C black, N blue, O red, Br brown, Cl green and Pd yellow.

The XRD analysis shown in Figure S15 suggests that about 90% of all the Br atoms on Pd^{II} remained intact and only 10% of them were replaced with Cl atoms, although the values of

occupancy may not be so accurate due to the moderate quality of the crystal data.

Crystal data of the core (MMF-Cl)

Crystal data for $(Pd_3\mathbf{L}Cl_{4.36}Br_{1.64})\cdot(Pd_3\mathbf{L}Cl_{3.93}Br_{2.07})\cdot(H_2O)_2$: $C_{84}H_{84}Cl_{8.31}Br_{3.69}N_{12}O_2Pd_6$, F_w = 2521.48, crystal dimensions 0.101 × 0.071 × 0.061 mm^3, monoclinic, space group $P2_1/c$, a = 20.2300(9), b = 53.5168(16), c = 14.3304(3) Å, β = 90.516(3)°, V = 15514.1(9) Å^3, Z = 4, ρ_{calcd} = 1.080 g cm^{-3}, μ = 1.805 mm^{-1}, T = 93 K, λ(MoKα) = 0.71073 Å , $2\theta_{max}$ = 50.0°, 111511/26700 reflections collected/unique (R_{int} = 0.1222), R_1 = 0.1699 ($I > 2\sigma(I)$), wR_2 = 0.4706 (for all data), GOF = 1.088, largest diff. peak and hole 2.424/–1.633 eÅ^{-3}. CCDC deposit number 1912585.

Note that, because the core crystal was cut off from the parent core-shell crystal with a micro-knife, the obtained small crystal was unavoidably damaged and the data quality was not high. However, it is enough to claim that the crystallinity of the core crystal is maintained. Since the reflection intensities of the higher angle region were considerably weak as mentioned above, all benzene rings were treated as rigid groups and restraints for thermal parameters such as SIMU, DELU and RIGU were applied to the framework to avoid the collapse of the structure during refinement. To discuss the degree of halogen exchange on each Pd ion, all halogen atoms were analysed as a disordered structure of Cl and Br. Hydrogen atoms of water molecules could not be located in the difference electron density maps.

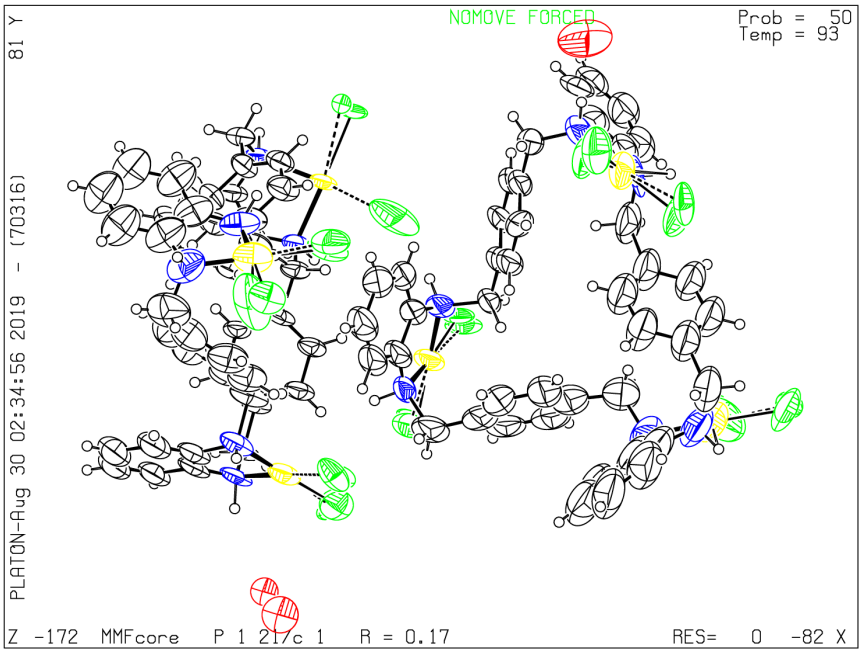

Figure S16. ORTEP drawings of the core (MMF-Cl) (50% probability level). Color: C black, N blue, O red, Cl/Br green and Pd yellow.

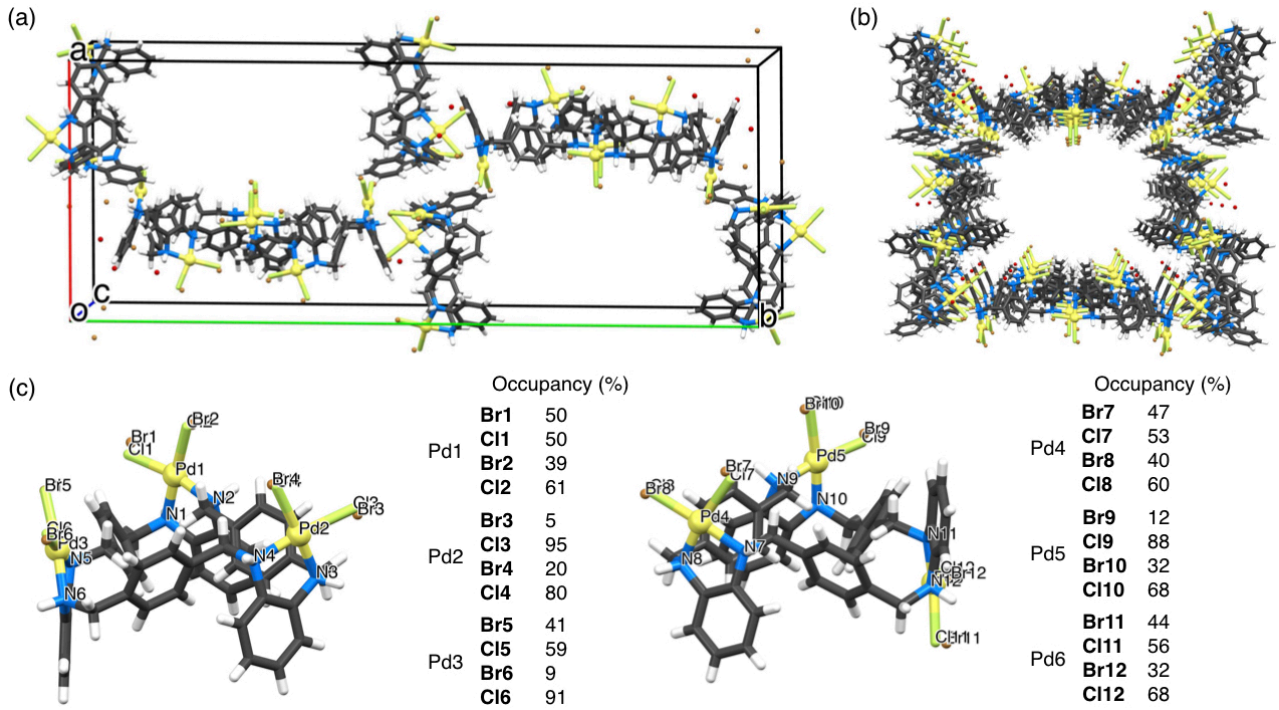

Figure S17. (a) Unit cell and (b) nano-channel structures of the core (MMF-Cl). (c) The *syn*- and *anti*-isomers and occupancy of halogen atoms on each Pd atom. Color: H white, C black, N blue, O red, Cl green, Br brown and Pd yellow.

The XRD analysis shown in Figure S17 suggests that about 70% of all the Cl atoms on Pd^{II} remained intact and only 30% of them were replaced with Br atoms, although the values of occupancy may not be so accurate due to the moderate quality of the crystal data.

Core-selective dye inclusion in MMF-Cl@MMF-Br

MMF-Cl crystals were immersed in a saturated aqueous solution of methyl orange and left at room temperature for several days. The resulting reddish orange crystals (Figure S18) were washed with water and acetonitrile in this order by decantation, and then mixed with an acetonitrile solution of macrocyclic ligand **L** and $PdBr_2(CH_3CN)_2$ ([**L**] = 0.28 mM, [$PdBr_2(CH_3CN)_2$] = 1.20 mM) prepared at 80 °C. Core-selectively dyed core-shell crystals were obtained after leaving this mixture at room temperature for several days (Figure S19).

Figure S18. Pictures of MMF-Cl crystals during the methyl orange dye incorporation process.

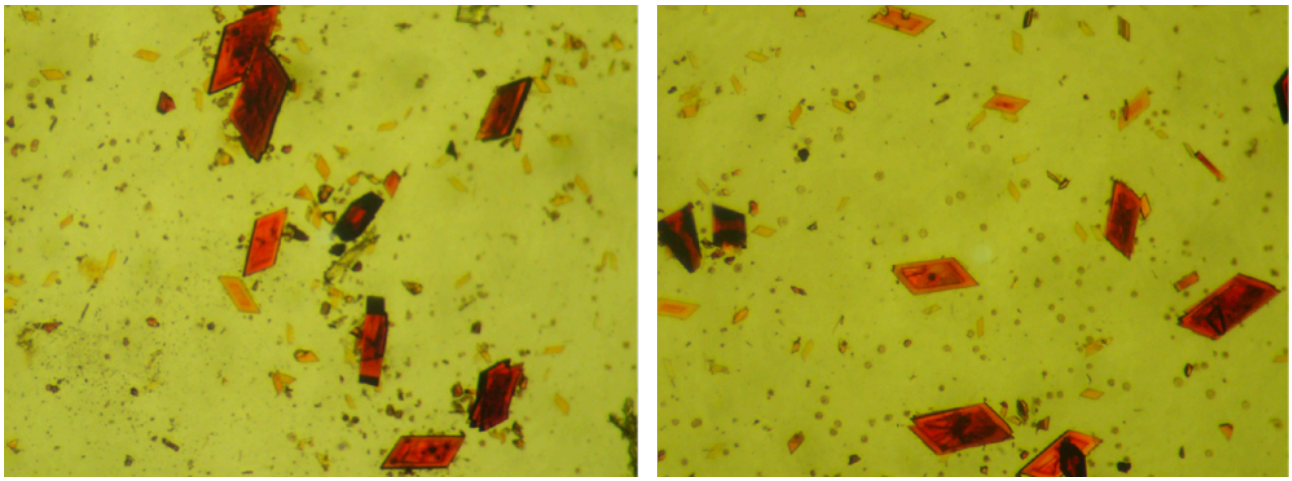

Figure S19. Pictures of core-shell MMF crystals whose cores selectively include methyl orange.

Anisotropic dye diffusion from the core to the shell domains

The resulting core-dyed crystals were left to stand at room temperature for 9 days in the crystallization solution of the shell, and then were observed with a microscope to check the anisotropic diffusion of methyl orange along the channels (Figure S20). Spatially selective dyeing was also supported by the plot profile of luminance (gray value) along the line part of the crystal (Figure S20a).

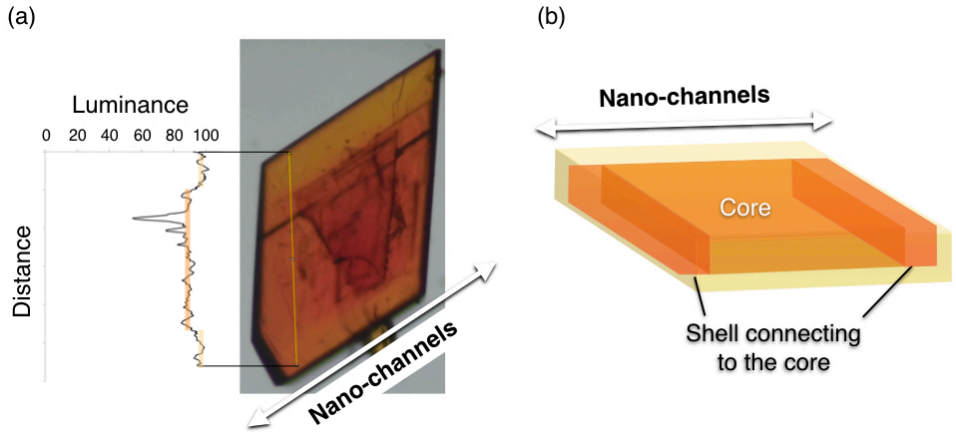

Figure S20. (a) Picture of anisotropic dye diffusion from the core to the shell of a core-selectively dyed crystal after 9 days and plot profile of luminance (gray value) along the line part. (b) Schematic representation of dye diffusion along the channels.

Reproducibility of the anisotropic diffusion of methyl orange was confirmed as follows. MMF-Cl crystals were soaked in an aqueous solution of methyl orange (saturated) for 2 days. After removing the supernatant and washing the crystals with water and acetonitrile, an acetonitrile solution of macrocyclic ligand **L** and $PdBr_2(CH_3CN)_2$ ([**L**] = 0.29 mM, [$PdBr_2(CH_3CN)_2$] = 1.3 mM) prepared at 80 °C was added to the crystals at room temperature, and then the mixture was left to stand for 4 days to grow shell crystals. Finally, some of the crystals were transferred to a glass plate and

covered with a fluorinated polymer (Fomblin Y). Pictures taken after several days showed anisotropic diffusion of methyl orange in some crystals (Figure S21).

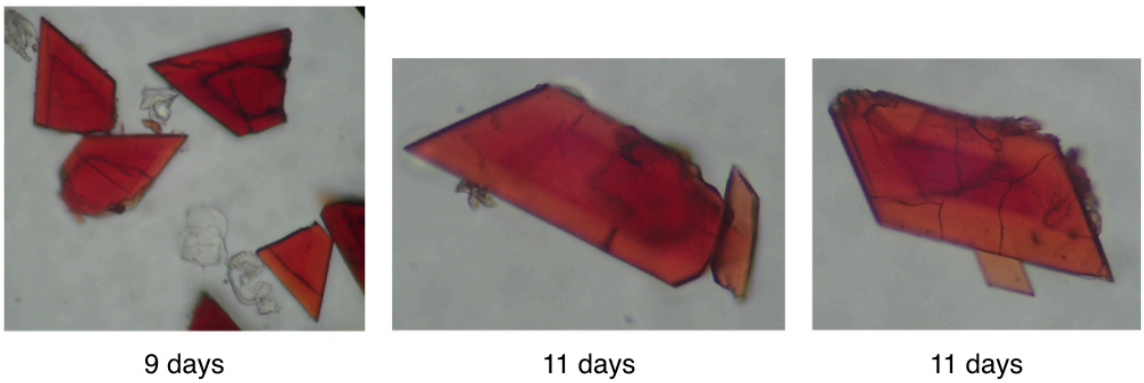

Figure S21. A picture of anisotropic dye diffusion from the core to the shell of core-selectively dyed crystals several days after initiating MMF-Br shell growth.

In addition, time-course observation of methyl orange diffusion was also examined as follows. MMF-Cl crystals were soaked in an aqueous solution of methyl orange (almost saturated) for 2 days. After removing the supernatant and washing the crystals with water and acetonitrile, an acetonitrile solution of macrocyclic ligand **L** and $PdBr_2(CH_3CN)_2$ ([**L**] = 0.26 mM, [$PdBr_2(CH_3CN)_2$] = 1.3 mM) prepared at 80 °C was added to the crystals at room temperature, and then the mixture was left to stand for 15 h to grow the shell crystals. The resulting core-shell crystals and the crystallisation solution were transferred to a slide glass, which was then covered by a thin glass plate with silicon grease. The slide glass was kept in acetonitrile to prevent crystal drying for several days (Figure S22).

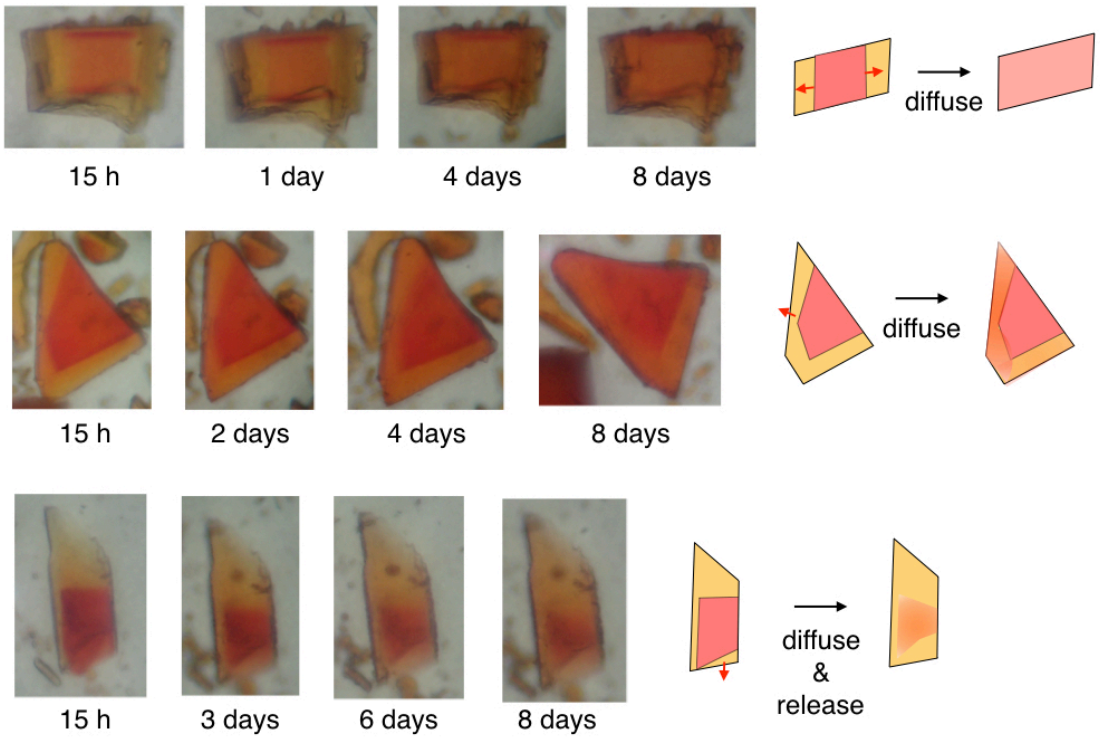

Figure S22. Time-course observation of dye diffusion and schematic representations of the diffusion or release of methyl orange. In the bottom case, the release of the dye might be due to the lack of the edge of the crystal.

References

1. S. Tashiro, R. Kubota and M. Shionoya, *J. Am. Chem. Soc.*, 2012, **134**, 2461–2464.

2. G. M. Sheldrick, *SHELXL-97, Program for refinement of crystal structure* (University of Göttingen, Göttingen, Germany, 1997); *Acta Cryst.*, 2008, **A64**, 112–122.